Thermochimica Acta 516 (2011) 79–87

Contents lists available at ScienceDirect

Thermochimica Acta

journal homepage: www.elsevier.com/locate/tca

Curing kinetics of a furan resin and its nanocomposites

Guadalupe Rivero [a], Valeria Pettarin [a], Analía Vázquez [b], Liliana B. Manfredi [a,*]

[a] Research Institute of Materials Science and Technology (INTEMA), National University of Mar del Plata, Juan B. Justo 4302, 7600 Mar del Plata, Buenos Aires, Argentina
[b] Polymer and Composite Material Group-INTECIN (UBA-CONICET)- Engineering Faculty, University of Buenos Aires, Las Heras 2214, 1127AAR Buenos Aires, Argentina

ARTICLE INFO

Article history:
Received 26 October 2010
Received in revised form
29 December 2010
Accepted 12 January 2011
Available online 26 January 2011

Keywords:
Furan resin
Clay
Nanocomposites
Differential Scanning Calorimetry
Curing kinetics

ABSTRACT

A furan resin was synthesized from furfural and phenol and it was expected to have similar properties to the commonly used phenolic resins because the former was obtained by the replacement of formaldehyde by furfural, reducing the dangerous formaldehyde emissions. In the present work, nanocomposites were obtained by the in situ addition of 2% of different types of clays to the furan resin to enhance the polymer performance. Montmorillonite natural clay Cloisite® Na^+ and the chemically modified ones, Cloisite® 30B and Cloisite® 10A were used. A clay dispersion comparison among the nanocomposites was performed.

The curing kinetics of the furan resin and its composites was characterized by Differential Scanning Calorimetry. Free kinetic models were applied in order to obtain and compare the activation energy of each process. Vyazovkin numerical analysis was found to provide the most accurate method to analyze the variation of the activation energy (E) with the reaction conversion.

Some differences arise in the activation energy vs. conversion profile among the materials studied. These differences were related to the variations in the viscosity and the chemical groups with the evolution of the curing reaction, followed by infrared spectroscopy. The nanocomposites containing the organically modified clays showed an additional peak in the last stage of the curing process due to parallel reactions including the beginning of the organic modifier decomposition.

1. Introduction

Furan resins are a likely alternative to phenolic resins because they can be obtained by replacing the toxic formaldehyde by furfural. As the global tendencies nowadays lead to the use of renewable resources for the development of new polymeric materials, furan resins could be an alternative because furfural can be easily obtained from a wide range of agricultural residues containing pentoses. So, it should be possible to obtain a material with excellent thermal and oxidative resistance, as phenolic resins, but reducing the contaminant formaldehyde emissions.

These kinds of thermosetting polymers are widely used in industrial applications; therefore, the state of curing and kinetic parameters is required in order to elucidate the best manufacturing process. Many complex reactions take place during the curing stage of thermosetting polymers, so this step determines the material's final properties and the study of the cure kinetics significantly contributes in the improvement of the final product performance and quality. Additionally, such systems do not allow deriving a mechanistic model based on chemical species balances because of the complicated simultaneous reactions involved [1]. Moreover, in many cases, even phenomenological or empirical models are still unsuitable to accurately describe the cure kinetics, and the traditional model-fitting methods may not be adequate.

In the last few decades, polymer-nanocomposites have gained worldwide research interest for developing materials with several improved properties by incorporation of nanoscaled particles into a polymer matrix. Clay mineral incorporated polymer nanocomposites have been widely studied [2] and it was found that the addition of those nanoparticles leads to chemical variations that may modify the polymer reaction mechanisms. As these changes affect the final properties of the resin, it is worth to study their effect on the kinetic parameters involved in the curing. In spite of the chemical characterization of different furan based resins being reported [3,4], their use in nanocomposites has not been widely published yet.

Differential Scanning Calorimetry (DSC) has been widely used to calculate the kinetic parameters of thermosetting curing reactions through measuring the overall extent of the chemical conversion by different methodologies. Isothermal and dynamic methods have been used to evaluate the degree of conversion (α), defined as the extent to which the highest achievable crosslinks have been formed in the reaction; as well as the conversion rate ($d\alpha/dt$) and the activation energy (E). Kissinger has proposed a method that can be used to calculate the activation energy of the overall curing process. Nev-

* Corresponding author. Tel.: +54 223 4816600; fax: +54 223 4810046.
E-mail addresses: avazquez@fi.uba.ar (A. Vázquez), lbmanfre@fi.mdp.edu.ar (L.B. Manfredi).

0040-6031/$ – see front matter © 2011 Elsevier B.V. All rights reserved.
doi:10.1016/j.tca.2011.01.022

Table 1
Characteristics of the clays incorporated in FNa, F30B and F10A resins.

Clay	Cloisite® Na^+ (CNa)	Cloisite®30B (C30B)	Cloisite®10A (C10A)
Organic modifier	None	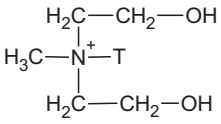	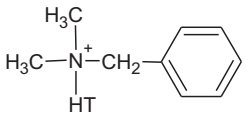

ertheless, since thermosetting systems are so complex and that E changes with α, isoconversional methods are the key to describe variations in the curing kinetics throughout the whole process. Isoconversional methods have been previously applied to the cure of many other thermosetting systems and require no knowledge of the reaction model.

In this work, Ozawa, Friedman, Ortega and Vyazovkin model-free kinetic methods were applied to generate consistent E profiles in function of α of a furan resin and its nanocomposites synthesized by the in situ addition of three types of montmorillonite clays. Neither of the applied methods requires knowledge of the conversion-dependence function $f(\alpha)$. The aim of this paper is to accomplish a comparison of different methods to determine the most accurate kinetic parameters that describe the curing processes of furan resins. Therefore, the curing kinetic profile of the furan resin was compared with the ones obtained from the nanocomposites in order to establish differences derived from the addition of nanoparticles.

2. Experimental

2.1. Materials

Phenol was molten into a reactor at 135 °C and the reaction media were adjusted with an aqueous solution of K_2CO_3 40% (w/v). Furfural was dropped in (1:1) molar proportion into phenol for 30 min and the temperature was maintained at 135 °C for 4 h to obtain F prepolymer resin. The prepolymer resins were heated to 110 °C and 12% of hexamethylentetramine (HMTA) was added as a catalyst. Once the mixture was homogeneous, the resins were cured by a temperature treatment up to 180 °C.

Nanocomposites were synthesized in a similar way but 2% of montmorillonite was added "in situ" to the melted phenol and the mixture was shaken for an hour before the addition of furfural. Three different montmorillonite type clays were used: natural purified Cloisite® Na^+ (FNa) and organically modified Cloisite® 30B (F30B) and Cloisite® 10A (F10A) (Southern Clay Products, USA). The chemical modifiers are shown in Table 1.

2.2. DSC measurements

Differential Scanning Calorimetry (DSC) is the most common method used to achieve thermal analysis of thermosetting resins. Unless there are secondary enthalpic events, it is possible to assume that the heat flow (dH/dt) is directly proportional to the reaction progress ($d\alpha/dt$) [5]. Dynamical and isothermal DSC methods were performed in the present work to analyze the curing kinetics of the furan resin and its nanocomposites.

2.2.1. Dynamic DSC methods

After the addition of the catalyst to the prepolymer, the samples were cured into a Shimadzu DSC-50 from room temperature to 250 °C, with dynamic scans at different heating rates: 2, 5, 10, 20 and 25 °C/min. The α value was determined as the ratio between the heat released up to a certain time t (ΔH_t) and the total heat of reaction (ΔH_{Dyn}) as follows: $\alpha = \Delta H_t/\Delta H_{Dyn}$.

Methods based on a unique heating rate is required to suppose a specific curing reaction mechanism or at least, to assume a particular kinetic model. As previously said, kinetic analyses of thermosetting resins are usually complex because simultaneous chemical reactions take place during the curing. So that, it is difficult to find a single model which represents the whole system.

Isoconversional methods assume that conversion (α_p) is constant at the reaction DSC peak and independent of the several heating rates used. In general, reaction rate may be described according to the progress of reaction and temperature by means of Eq. (1):

$$\frac{d\alpha}{dt} = kf(\alpha) \tag{1}$$

Considering that the rate constant (k) follows Arrhenius law for a given heating rate $\beta = (d\alpha/dt)/(d\alpha/dT)$, Eq. (2) is obtained:

$$\beta\frac{d\alpha}{dT} = A\exp\left(\frac{-E}{RT}\right)f(\alpha) \tag{2}$$

where A is the pre-exponential factor, R is the gas universal constant and $f(\alpha)$ is the function that describes the kinetic model. Deriving and equalling $d^2\alpha/dT^2 = 0$ for the peak temperature, Eq. (3) is obtained:

$$\ln\left(\frac{\beta}{T_P{}^2}\right) = \ln\left(\frac{AR}{Ef(\alpha)}\right) - \frac{E}{R}\frac{1}{T_P} \tag{3}$$

A graph of $\ln(\beta/T_P^2)$ vs. $(1/T_P)$ led to a decreasing straight line whose slope involves the activation energy value (E) for the global reaction. This procedure was first developed by Kissinger [6]. It is clearly seen that this method does not require to know $f(\alpha)$. It just presupposes that the reactive process has the same reaction mechanism for a given conversion, independent of the curing temperature. Nevertheless, it does not detect E variation with α and therefore, other methods become more accurate for these kinds of reactions.

Ozawa method provides a simple expression given by Eq. (4), obtained by the integration and rearrangement of Eq. (1). It allows calculating E for each conversion degree by the slope of the graph of $(\ln\beta)$ vs. $1/T_i$ [7]:

$$E = \frac{-R}{1052}\frac{\Delta\ln\beta}{\Delta(1/T_i)} \tag{4}$$

However, this method has been criticized because no changes in E are assumed during the numerical integration of Arrhenius equation [8]. If the results show a change in E during the progress of reaction, the variable separation used in this method becomes invalid. Rigorously, isoconversional methods should be only used to infer Eq. (2) validity and then they would provide a precise description of the reaction kinetics.

Friedman isoconversional method uses a logarithmic rearrangement of Eq. (2), which provides E by the slope of the graph of $\ln(d\alpha/dt)$ vs. $1/T$ at each specific degree of cure (α), according to Eq. (5):

$$\ln\left[\beta_i\left(\frac{d\alpha}{dT}\right)_{\alpha,i}\right] = \ln[f(\alpha_i)A_\alpha] - \frac{E_\alpha}{R}\frac{1}{T_{\alpha,i}} \tag{5}$$

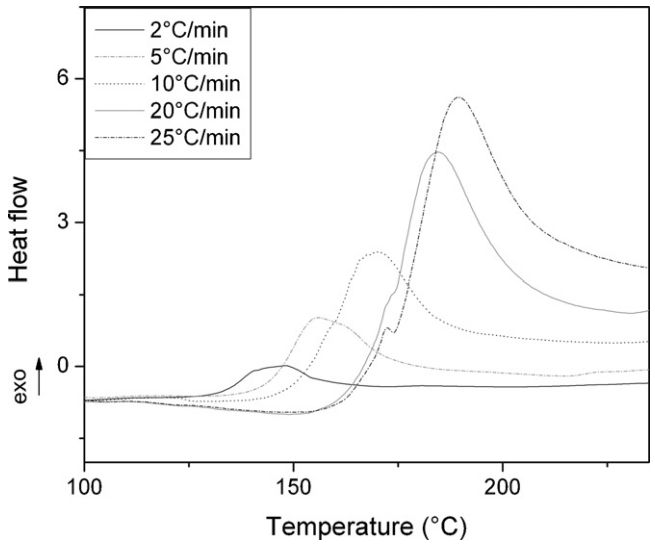

Fig. 1. Curing peak of the F resin from DSC dynamic scans at different heating rates.

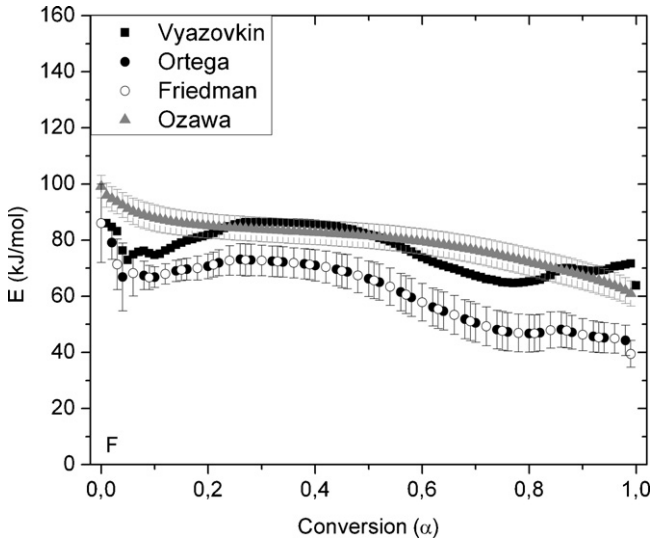

Fig. 3. F resin E profile obtained by Vyazovkin (■); Ortega (●); Friedman (○) and Ozawa (▲) methods with $\Delta\alpha = 0.01$.

Although no approximations are introduced in Eq. (5), Friedman method is affected by significant numerical instability and noise interference because it employs instantaneous rate values and uses the differential term $d\alpha/dt$ in the numerical calculus [9]. Therefore, Vyazovkin method was developed to eliminate the systematic error in E_α when it varies with α [10].

Vyazovkin [10] has developed an advanced non-linear procedure that performs integrations over small conversion intervals, $\Delta\alpha \approx 0.01$, where E is considered constant. Then, for a series of n experiments at different heating rates, E is determined for each interval as the value that minimizes the function given by Eq. (7). Systematic errors associated with major integrations are then minimized by this method [11]:

$$J[E_\alpha, T(t_\alpha)] = \int_{t_\alpha - \Delta\alpha}^{t_\alpha} \exp\left(\frac{-E_\alpha}{RT(t)}\right) dt \tag{6}$$

$$\sum_{i=1}^{n} \sum_{j \neq i}^{n} \frac{J[E_\alpha, T_i(t_\alpha)]}{J[E_\alpha, T_j(t_\alpha)]} \tag{7}$$

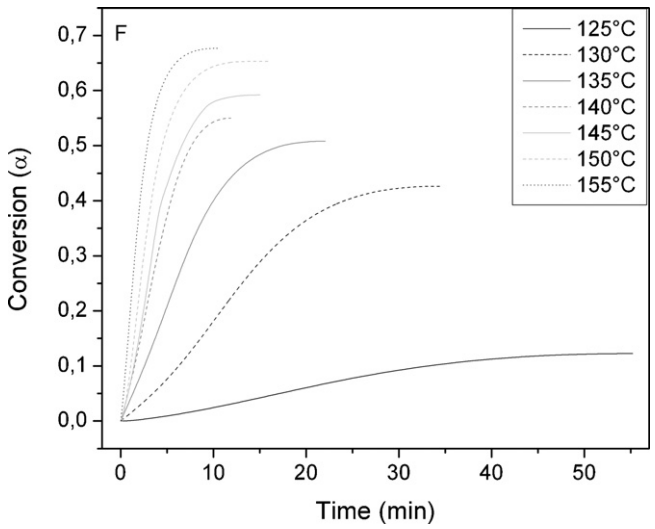

Fig. 2. Conversion of F resin vs. time from isothermal scans.

Ortega proposed an average linear integration method [12], which performs integrations over small temperature intervals. Then, the temperature integral is approximated by the mean value theorem and E is assumed constant only in a small $\Delta\alpha$ range. The method precision is limited by the interval magnitude. Hence, for a given α, Eq. (8) led to E by the slope of the graph of $\ln(\beta_i/\Delta T_{\alpha,i})$ vs. $1/T_{\alpha,i}$:

$$\ln\left(\frac{\beta_i}{\Delta T_{\alpha,i}}\right) = Const - \frac{E_\alpha}{R}\frac{1}{T_{\alpha,i}} \tag{8}$$

2.2.2. Isothermal DSC methods

Curing reactions were monitored in time into a Pyris-DSC, at constant temperatures. In these cases, the total conversion reached at each temperature is calculated by the ratio of the reaction peak at a given temperature (ΔH_T) and the total reaction peak area (ΔH_{Dyn}), which is determined by a dynamic DSC scan that assures an almost complete cure: $\alpha_T = \Delta H_T/\Delta H_{Dyn}$.

2.3. Gelation times

Gelation is an irreversible transformation of materials into a gel conformed of a unique 3D-interconected molecule. These changes take place at a characteristic reaction conversion called gel point, which depends on the functionality, reactivity and stoichiometry of the reagents. It was experimentally determined by registering how long does a wire last to get trapped into a thin glass tube containing the sample of the material at a fixed temperature [13]. If Eq. (2) is assumed to be valid, the time to gel may be expressed by Eq. (9):

$$t_{gel} = \frac{1}{A}\exp\left(\frac{E}{RT}\right)\int_0^{x_{gel}} \frac{dx}{f(x)} \tag{9}$$

If x_{gel} does not depend on temperature, it is possible to estimate E from the slope of the linear graph of $\ln(t_{gel})$ vs. $1/T_c$ [13].

2.4. FTIR measures

The curing reaction of the furan resin and the nanocomposites was monitored in situ by Fourier Transform Infrared (FTIR) spectroscopy. Spectra were obtained in a Mattson Genesis II, transmission mode, equipped with a heating furnace. Spectra were scanned from 600 to 4000 cm^{-1} from ambient temperature to

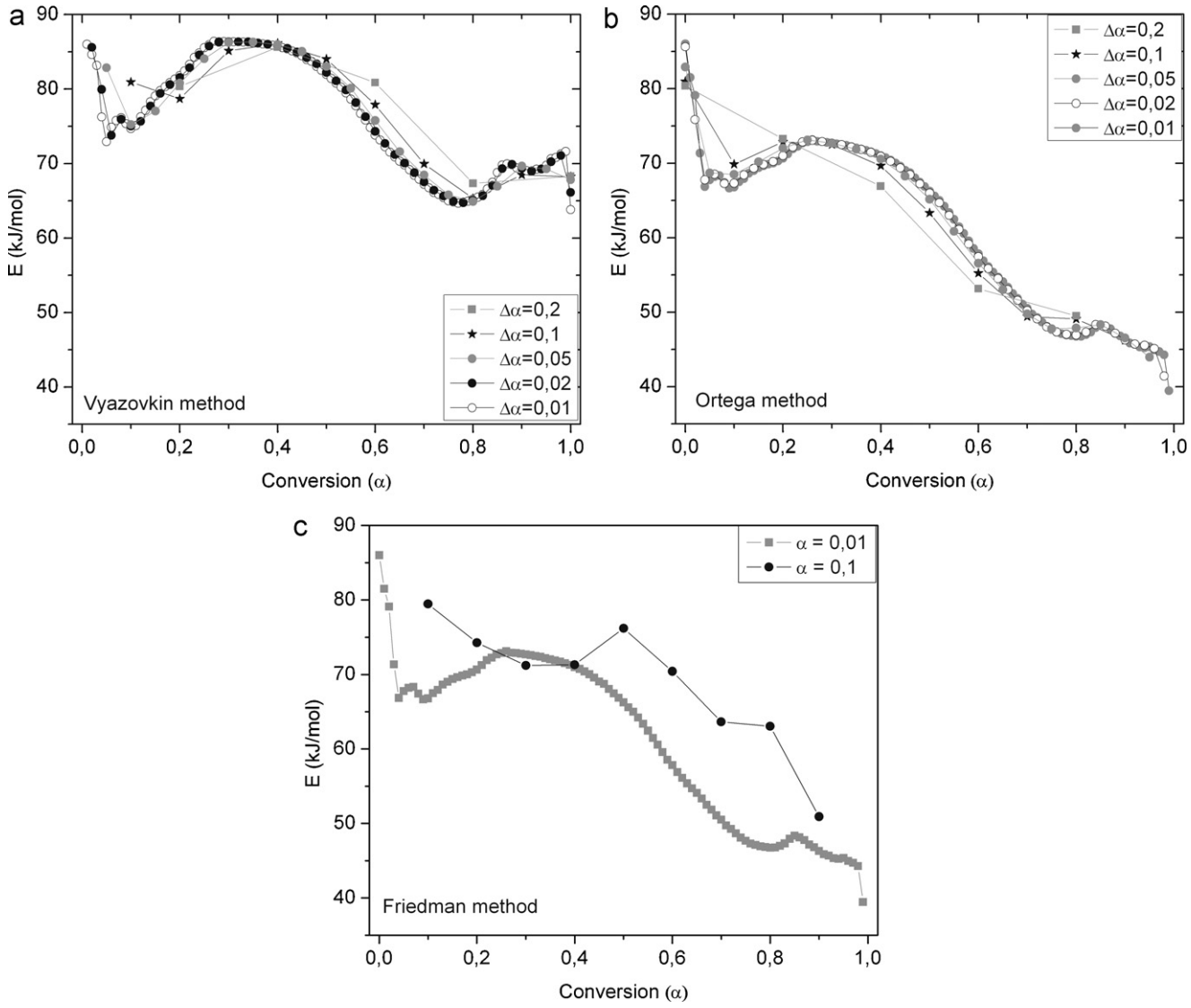

Fig. 4. *E* profile obtained with different $\Delta\alpha$ by (a) Vyazovkin, (b) Ortega and (c) Friedman methods.

180 °C, every 10 °C, at a heating rate of about 2 °C/min. For comparison purposes, spectra were normalized with the intensity of the band at 1595 cm^{-1} in every case. This band was assigned to the C=C benzene ring stretching and its intensity was expected to remain constant for all the samples [14].

2.5. Clay dispersion analysis

X-ray diffraction (XRD) analyses of the composites were performed in a Philips PW 1710 diffractometer (45 kV and 30 mA) at 2°/min, with a Cu K_α radiation (λ = 1.54 Å).

Transmission electron microscopic (TEM) images of the samples were obtained with a JEOL 100 CX II at 80 kV of acceleration voltage. All samples were ultramicrotomed at room temperature to give sections with a nominal thickness of 100 nm.

3. Results and discussion

3.1. F resin curing kinetics

Fig. 1 displays the curing dynamic DSC thermograms at several reaction rates that were employed to build the furan resin (F) curves of conversion degree against temperature. α vs. time curves that were built from isothermal essays performed at temperatures lower than the maximum peak are shown in Fig. 2.

x_{gel} values, calculated from isothermal α–T curves, were found to be almost independent of temperature so that gelation can be assimilated to an isoconversional principle [15,16]. An estimated value of an apparent *E* was calculated from the slope of the linear graph of $\ln(t_{gel})$ vs. $1/T_c$, assuming Arrhenius Equation (2) as valid. The Kissinger method was also applied and a global *E* was determined from the slope of a linear graph. Both values are shown in Table 2. These global results actually differ from each other though excellent linear correlations ($R > 0.99$) were obtained, indicating that *E* may vary during reaction.

Table 2
Activation energy (*E*) of F resin obtained by a gelation analysis and the Kissinger method.

Method	Gelation analysis	Kissinger method
Global *E* (kJ/mol)	88.0	72.5
Linear correlation coefficient (*R*)	0.995	0.986

The variation of E with α was calculated with the remaining methods using $\Delta\alpha = 0.01$. Results are compared in Fig. 3.

Plots showed a good linear correlation ($R > 0.98$) when Ozawa method was applied to the experimental results indicating that E values are independent of the selected range of heating rates. Nevertheless, Eq. (4) has been derived by assuming no changes in the kinetic model nor in E all over the reaction [8] and the solution to the exponential integral is calculated by Doyle's approximation (additional information can be found elsewhere) [17]. However, these assumptions become invalid since the profile of the Ozawa E curve is not constant in the whole range of conversion, as shown in Fig. 3.

The curves in Fig. 3 evidenced that Friedman and Vyazovkin methods lead to profiles more sensitive to changes in the cure mechanism. Although the profile tendency is similar among methods, there are differences in the absolute values that may be due to the mathematical calculus that led to each numerical expression and the instabilities of Friedman method [18]. In fact, Wang et al. [9] found that more accurate E_α functions were obtained with Friedman and Vyazovkin methods as close-form approximations are not used.

Ortega integrates the rate equation over small ranges with respect to time and E variation with α is detected. It is noticeable that the curve obtained by Friedman method matches exactly with the one acquired by Ortega method when $\Delta\alpha = 0.01$. This fact is expected because of the limitation of the α interval to validate the assumption of constant E in a given interval. When the term $\Delta\alpha$ in Ortega method becomes smaller, the α interval ($\Delta\alpha$) tends to the differential term ($d\alpha$) used by Friedman. So that the key factor to get an accurate E profile seems to be the correct selection of data intervals.

Therefore, the accuracy and sensibility of these methods were optimised by the evaluation of the error-minimizing variables during the numerical calculus. For this purpose, E curves were calculated all over again with different $\Delta\alpha$. As it is known, the choice of $\Delta\alpha$ is generally a compromise between accuracy and noise smoothing. It was found that effectively, the curve tendency and the absolute values are notably affected by the selected conversion interval as seen in Fig. 4. Consequently, the experimental results confirmed that the precision of these methods strongly depends on the precise evaluation of $\Delta\alpha$ or $T_{\alpha\text{-}\Delta\alpha}$ and T_α [12]. In general, E profiles remain fairly constant if a maximal $\Delta\alpha = 0.05$ is used. Nevertheless, if isoconversional methods are applied in order to reveal changes in the curing kinetics or elucidate curing mechanisms, it is suitable to employ at least a maximal $\Delta\alpha = 0.02$ to properly define eventual peaks. A further diminish in calculus interval to $\Delta\alpha = 0.01$ did not increase noise nor a significant improvement in curves was observed. Therefore $\Delta\alpha = 0.02$ was selected as the best interval for practical purposes.

In order to evaluate the accuracy of the different methods, experimental curves of conversion vs. temperature were compared with the predicted curves according to obtained E. Fig. 5 shows the match of the different method predictions with the experimental F curves. A correlation parameter was calculated as the difference between experimental and predicted curves by Eq. (10). Correlation parameter C varies between 0 and 1, representing 1 as an exact match. It was found that Vyazovkin predictions provided the best match with the experimental curves (Table 3):

$$C = 1 - \frac{\left|T_{\text{measured}} - T_{\text{predicted}}\right|}{T_{\text{measured}}} \quad (10)$$

3.2. Nanocomposite curing kinetics

The four isoconversional methods previously mentioned were used to obtain the E profile curves for the nanocomposites containing the different clays (Fig. 6). Ozawa curves resulted again suitable

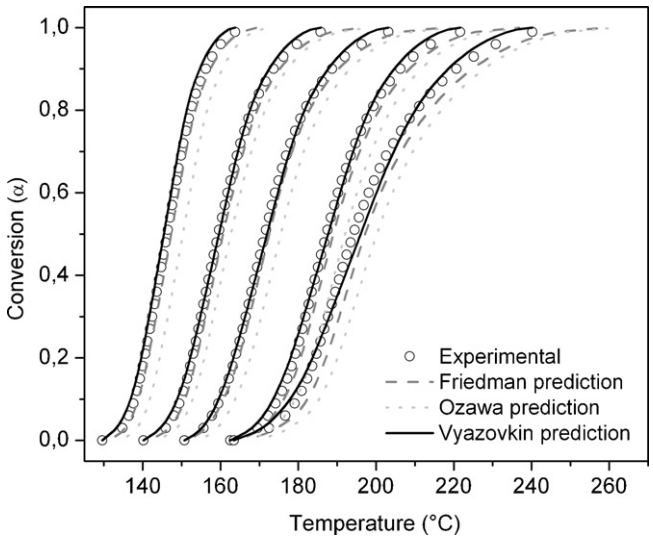

Fig. 5. Conversion–temperature curves of the F resin approached with the different method predictions.

Table 3
Adjusting parameters of the correlation between the experimental and the predicted curves for F resin.

Method	R
Vyazovkin	**0.9948**
Friedman	0.9832
Ortega	0.9832
Ozawa	0.9704

only to get an estimation of the global E value while the other methods provided a more detailed description of E changes during the reaction progress. Although there are several differences in the relative numerical values, the E profile curves maintain a similar tendency with Friedman, Ortega or Vyazovkin method. The shape of the curves obtained by these methods reveals meticulous changes in the curing mechanisms. Certainly, complex reactions involving various simultaneous reactions or changes in the limiting step produce differences in E. In general, an increasing E function indicates competition between parallel reactions. Concave decreasing E curves could be characteristic of reversible stage reactions; while convex ones reveal a limiting stage change [9]. Once again, Vyazovkin model provided the best adjusting parameters for all materials (Table 4).

Consequently, Vyazovkin curves were used for comparative purposes. It was reported [15] that when partial heat corresponds to heights in a thermogram curve which are less than 5% in relation to the maximum peak height, significant error affects the kinetic parameters of that range. Therefore, the initial measures until $\alpha \sim 0.02$ can become deviated so that they were not considered in the following analysis.

Fig. 7 compares the E profiles for each material curing process. Several authors have reported an initial decrease of E linked to a

Table 4
Nanocomposites adjusting correlation parameters (R) between the experimental and predicted curves obtained by each model.

Model	R		
	FNa	F10A	F30B
Vyazovkin	**0.9928**	**0.9819**	**0.9820**
Friedman	0.9667	0.9404	0.9587
Ortega	0.9667	0.9404	0.9587
Ozawa	0.9687	0.9864	0.9664

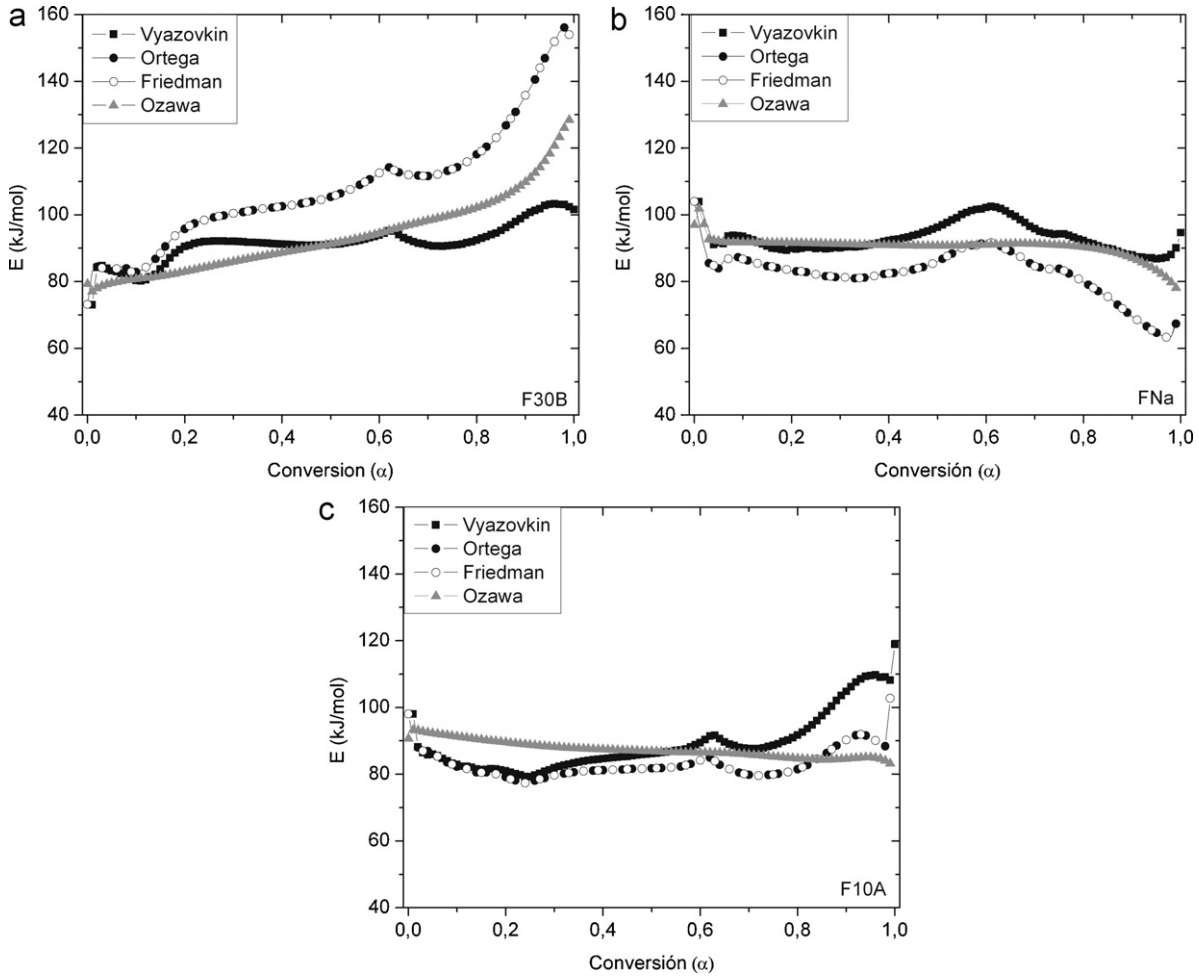

Fig. 6. *E* profile vs. conversion, obtained by the four methods for nanocomposites: (a) F30B, (b) FNa and (c) F10A.

viscosity-related mechanism [19,20]. In fact, the initial curvature exhibits a more marked decreasing shape for the nanocomposites, due to the increase of viscosity caused by the clay introduction.

Afterward, the effect of higher viscosity which leads to a downward dependence curve is more or less counteracted by the continuation of addition and condensation reactions that keep on increasing the crosslinking and the conversion degree [21]. This sequence of addition reactions of furfural to phenol takes place at first, during the prepolymer synthesis, leading to chemical species capable of substituting another activated phenol positions or reacting among each other generating ether bridges [21]. The processes continue during the curing stage, increasing the substitution extent and the crosslinking degree. These kinds of competitive reactions lead to upward tendency curves.

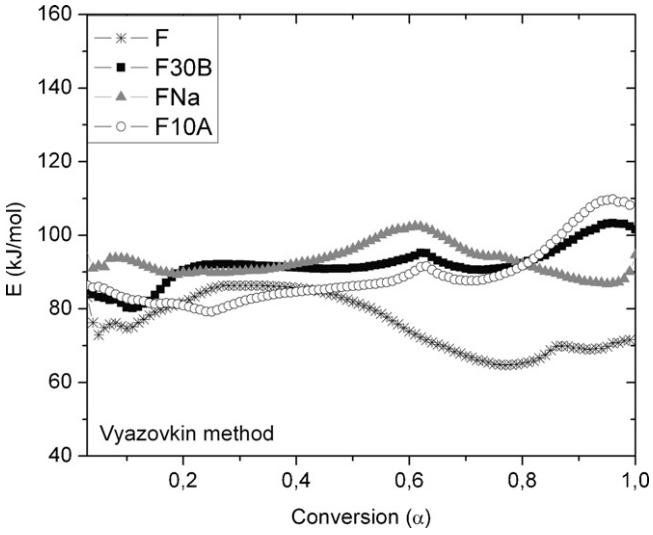

Fig. 7. *E* profile curves obtained by Vyazovkin method for each material.

After $\alpha \approx 0.1$, these crosslinking reactions become preponderant in the F resin, which is expected to be the least viscous material so that it has no added clay. As a result, the F profile exhibits a wide peak. Besides, the F30B resin curve shows a notable increase at the same conversion degree, favored by of –OH groups provided by the modified clay, which are capable of taking part in the addition and condensation reactions. This rise is certainly slight for F10A resin and the upward dependence may be actually in competition with the descending tendency caused by the viscosity raise. Moreover, the similar intensity of these opposite factors causes that *E* maintains about ≈90 kJ/mol in FNa. A previous work determined that FNa prepolymer reached the most advanced conversion degree in the synthetic step, as evidenced by the highest amount of –CH– bridges related to the crosslinking extent [21]. As a result, the upward dependence does not become dominant because there are not so many chemical groups left free to react. In conclusion, the nanocomposite curves level off probably because of the competition of opposite tendencies.

As conversion continues, the curves increase to reach a maximum. This may indicate that addition reactions are limited and

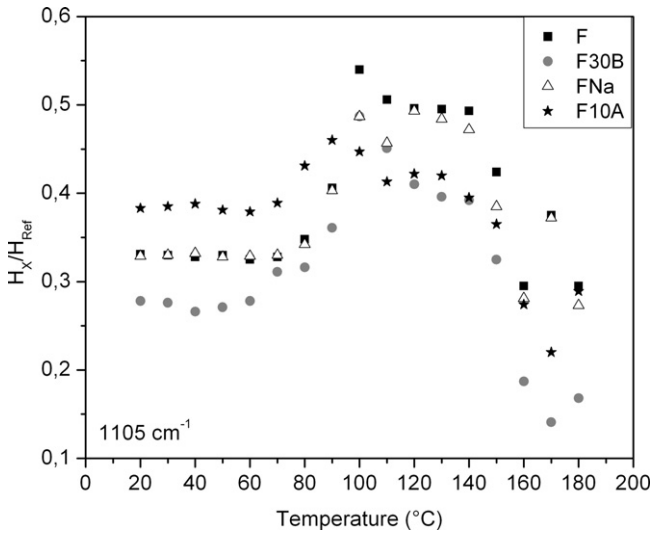

Fig. 8. Relative intensity of the 1105 cm^{-1} band during the curing for each material, related to the evolution of ether bridges.

almost completed [22]. In addition, this progressive increase at relatively high conversion may be due to the simultaneous action of new processes initiated with different reaction mechanisms. A similar deviation of the *E* decreasing track at high conversion degree was previously reported [17,19,22]. At this stage, the most likely process was the ether bridge decomposition reactions to form more stable C–H bridges. However these later processes take place at an earlier conversion ($\alpha \approx 0.6$) in the nanocomposites probably enhanced by the clay addition. In contrast, F resin exhibits a similar peak only since conversion is about $\alpha \approx 0.85$.

Ether bridge progress was corroborated by following the evolution with curing temperature of the band assigned to the symmetric C–O stretching at 1105 cm^{-1} [23] for each material. It is observed in Fig. 8 that in all cases, ether bridge formation occurs at low temperatures and its relative quantity is maintained practically until 140 °C is reached. From this temperature, ether bridges are notably decreased. Provided by the adequate conversion – temperature curves (Fig. 5) obtained also at 2 °C/min, it is possible to correlate the functional group evolution with temperature as well as with the changes in *E*.

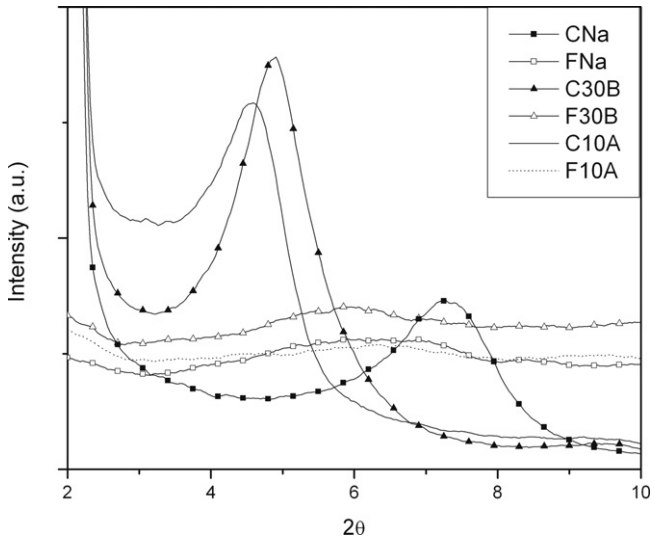

Fig. 9. DRX curves of the clays and the nanocomposites.

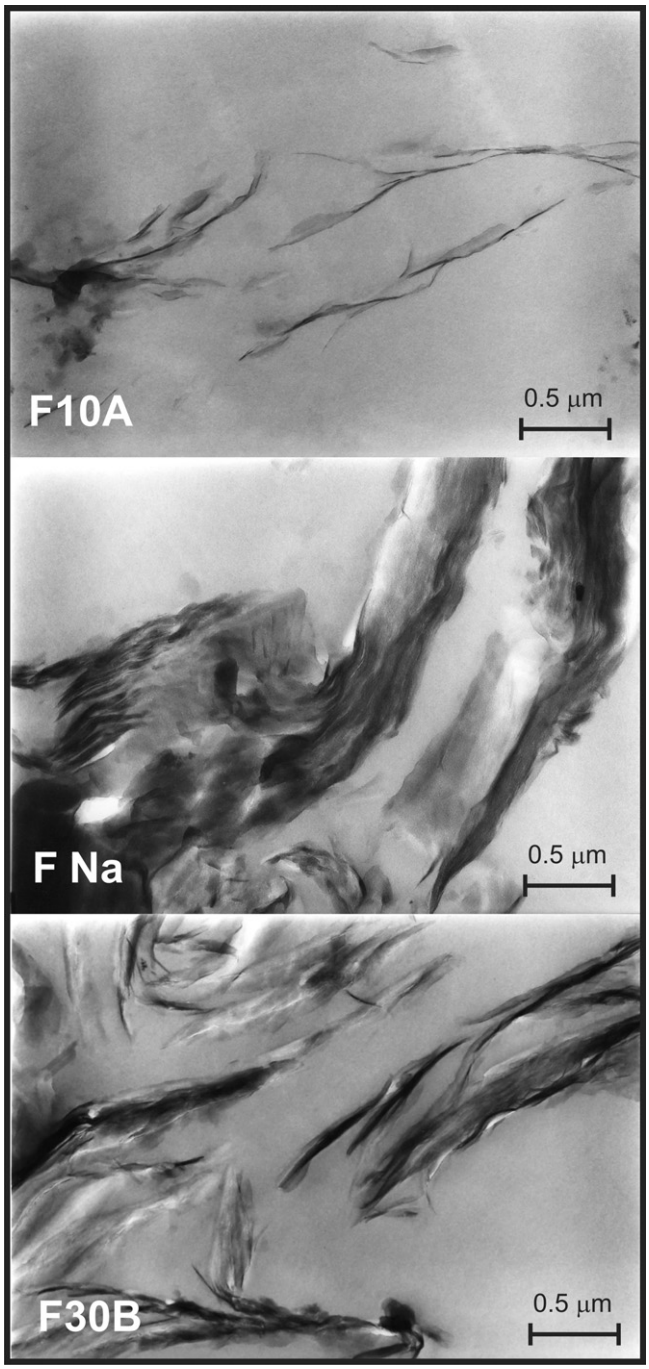

Fig. 10. TEM images of the nanocomposites.

In fact, although the conversion rate is different for each material, the *E* peak appears at approximately 150–155 °C in all cases. It means that at this temperature the ether bridges actually decompose, forming –CH– bridges and releasing furfural. Nevertheless, remarkable differences exist as F resin certainly reached a higher conversion degree when this process takes place.

Later, the curves of *E* vs. α (Fig. 7) decrease because of the transition in the kinetic control from chemical to diffusional. When the cure temperature equals the glass transition temperature of a system, the material vitrifies and the polymerization is practically stopped because the molecular mobility becomes dramatically decreased. This transition should diminish the effective *E* with increasing α [24].

With regard to this, two different behaviors can be described in the last stage. On the one hand, F and FNa resins exhibit a clearly decreasing shape consistently with the diffusion regime explained before. The relative differences between the numerical E values may be due to the mobility impediment caused by the clay sheets that may act as physical barriers in FNa, which lead to 20% higher E values in the last stages.

On the other hand, the resins with organically modified clays reveal a final E increment since $\alpha \approx 0.75$. In fact, an upward shape reveals again multiple parallel reactions almost certainly related to the beginning of the organic modifier degradation reactions that occur since that temperature range [25,26].

In order to analyze the clay dispersion in the polymer matrix, DRX analysis (Fig. 9) and TEM image analysis (Fig. 10) were performed. It was observed that the clay layers are intercalated in the matrix even if there are dispersion differences probably because of the chemical nature of each filler. The interlayer distance of the unmodified clay in FNa was enhanced compared to the pristine clay, as the basal peak in DRX profile was shifted toward lower angles, but the sheets showed zones with more agglomeration as seen by TEM. In spite of the diminution of the gallery gap in the modified clays, the final interlayer distance was similar among all materials. TEM images reveal that the sheets are intercalated, being C10A the best dispersed filler. As the MMT is quite well dispersed, its large aspect ratio does not hinder significantly the mobility of the reactive species. On the contrary, chains are allowed to crosslink and as previously discussed, some processes are even favored in the presence of these nanofillers.

No changes were reported in the cure mechanisms of thermosetting polymer matrix after the addition of different types of conventional fillers [27,28]. Nevertheless different cure conditions were found near the filler/polymer interface due to the presence of a coupling agent in the filler [29]. In the case of nanoreinforcements, the interfacial area is considerably major than in traditional fillers, so it could explain the significant differences in the cure mechanisms compared with the neat polymer that were observed in this work.

4. Conclusions

Activation energy of the curing process as a function of conversion was calculated by applying different isoconversional methods to a furan resin. It was stated that Ozawa's method is not suitable for this system because as E changes during the reaction, the suppositions assumed became invalid.

Nevertheless, Vyazovkin numerical analysis provides the most accurate method to analyze the E variation with the conversion degree. Although Ortega methods involve simpler mathematical calculation, its precision is more affected by the selected $\Delta\alpha$. Friedman method supplies a good profile if conversion intervals are small enough so that the resulting curves match Ortega ones. However, noise interference may introduce errors associated with the instantaneous rate values employed in the calculus and the predicted curve does not correlate with the experimental points as well as Vyazovkin predictions do.

Once the most suitable method was established for the furan resin, each nanocomposite E profile was obtained applying this method. Although an initial E decrease was attributed to the viscosity increment in all the studied systems, this tendency was counteracted in different ways by an upward tendency related to the continuation of addition and condensation reaction. These reactions became preponderant in the furan resin, while the nanocomposite E curves level off because of the competition of both opposite trends. However, several profile differences arise among each other. This fact could be explained as a result of the different chemical groups containing the clay modifiers as well as the differences in the crosslinking degree achieved previously throughout the prepolymer synthesis.

Besides, the appearance of a slight peak in the E profiles revealed some new processes related to the decomposition of ether bridges. These observations were corroborated by FTIR measures, and the materials were compared based on the conversion and temperature at which processes occur in each case. Finally, F30B and F10A resins exhibit an additional increase of E in the final stage, probably related to the beginning of the organic modifiers decomposition.

The complete kinetic analysis performed in this work allowed to study the way the nanoreinforcements actually modified the furan polymer matrix cure mechanisms.

Acknowledgements

The authors gratefully acknowledge the financial support from the National Research Council of Argentina (CONICET) - PIP 014 and the National University of Mar del Plata.

References

[1] M.V. Alonso, M. Oliet, J.M. Perez, F. Rodriguez, J. Echeverria, Determination of curing kinetic parameters of lignin–phenol-formaldehyde resol resins by several dynamic differential scanning calorimetry methods, Thermochim. Acta 419 (2004) 161–167.
[2] F. Hussain, M. Hojjati, M. Okamoto, R. Gorga, Polymer-matrix nanocomposites, processing, manufacturing, and application: an overview, J. Compos. Mater. 40 (2006) 1511–1565.
[3] A. Pizzi, H. Pasch, C. Simon, K. Rode, Structure of resorcinol, phenol and furan resins by MALDI-TOF Mass spectrometry and ^{13}C NMR, J. Appl. Polym. Sci. 92 (2004) 2665–2674.
[4] A. Gandini, M.N. Belgacem, Furans in polymer chemistry, Prog. Polym. Sci. 22 (1997) 1203–1379.
[5] F. Boey, W. Qiang, Experimental modeling of the cure kinetics of an epoxy-hexaanhydro-4-methylphthalicanhydride (MHHPA) system, Polymer 4 (2000) 2081–2094.
[6] H.E. Kissinger, Reaction kinetics in differential thermal analysis, Anal. Chem. 9 (11) (1957) 1702–1706.
[7] T. Ozawa, A new method of analyzing thermogravimetric data, Bull. Chem. Soc. Jpn. 38 (1) (1965) 1881–1886.
[8] J.M. Criado, P.E. Sánchez-Jimenez, L.A. Pérez-Maquedaet, Critical study of the isoconversional methods of kinetic analysis, J. Therm. Anal. Calorim. 92 (1) (2008) 199–203.
[9] J. Wang, M. Laborie, M. Wolcott, Comparison of model-free kinetic methods for modeling the cure kinetics of commercial phenol-formaldehyde resins, Thermochim. Acta 439 (2005) 68–73.
[10] S. Vyazovkin, Model-free kinetics: staying free of multiplying entities without necessity, J. Therm. Anal. Calorim. 83 (1) (2006) 45–51.
[11] S. Vyazovkin, Modification of the integral isoconversional method to account for variation in the activation energy, J. Comput. Chem. 22 (2) (2001) 178–183.
[12] A. Ortega, A simple and precise linear integral method for isoconversional data, Thermochim. Acta 474 (2008) 81–86.
[13] J.P. Pascault, H. Sauteraeau, J. Verdu, R.J.J. Williams, Thermosetting Polymers, Marcel Dekker, New York, 2002.
[14] L.B. Manfredi, D. Puglia, J.M. Kenny, A. Vázquez, Structure–properties relationship in resol/montmorillonite nanocomposites, J. Appl. Polym. Sci. 104 (5) (2007) 3082–3089.
[15] M.V. Alonso, M. Oliet, J. Garcia, F. Rodriguez, J. Echeverria, Gelation and isoconversional kinetic analysis of lignin–phenol-formaldehyde resol resins cure, Chem. Eng. J. 122 (2006) 159–166.
[16] J.M. Perez, M. Oliet, M.V. Alonso, F. Rodriguez, Cure kinetics of lignin-novolac resins studied by isoconversional methods, Thermochim. Acta 487 (2009) 39–42.
[17] G. He, B. Riedl, Phenol–urea–formaldehyde cocondensed resol resins: their synthesis, curing kinetics, and network properties, J. Polym. Sci. Part B: Polym. Phys. 41 (2003) 1929–1938.
[18] M. Maciejewski, Computational aspects of kinetics analysis. Part B. The ICTAC Kinetics Project—the decomposition of calcium carbonate revisited, or some tips on survival in the kinetics minefield, Thermochim. Acta 355 (2000) 145–154.
[19] A. Tejado, G. Kortaverria, J. Labidi, J.M. Echeverria, I. Mondragon, Isoconversional kinetic analysis of novolac-type lignophenolic resins cure, Thermochim. Acta 471 (2008) 80–85.
[20] S. Vyazovkin, S. Sbirrazzuoli, Effect of viscosity on the kinetics of initial cure stages, Macromol. Chem. Phys. 201 (2) (2000) 199–203.
[21] G. Rivero, A. Vázquez, L.B. Manfredi, Synthesis and characterization of nanocomposites based on furan resins, J. Appl. Polym. Sci. 117 (3) (2010) 1667–1673.

[22] G. He, B. Riedl, A. Ait-Kadiet, Curing process of powdered phenol-formaldehyde resol resins and the role of water in the curing systems, J. Appl. Polym. Sci. 89 (2003) 1371–1378.
[23] K. Roczniak, T. Biernacka, M. Skarżyński, Some properties and chemical structure of phenolic resins and their derivatives, J. Appl. Polym. Sci. 28 (2) (2003) 531–542.
[24] N. Sbirrazzuoli, S. Vyazovkin, Learning about epoxy cure mechanisms from isoconversional analysis of DSC data, Thermochim. Acta 388 (2002) 289–298.
[25] A. Leszczynska, J. Njuguna, K. Pielichowski, J.R. Banerjee, Polymer/montmorillonite nanocomposites with improved thermal properties. Part I. Factors influencing thermal stability and mechanisms of thermal stability improvement, Thermochim. Acta 453 (2007) 75–96.
[26] L. Cui, D.M. Khramov, C.W. Bielawski, D.L. Hunter, P.J. Yoon, D.R. Paul, Effect of organoclay purity and degradation on nanocomposite performance. Part1. Surfactant degradation, Polymer 49 (2008) 3751–3761.
[27] D. Olmos, A.J. Aznar, J. Baselga, J. González-Benito, Kinetic study of epoxy curing in the glass fiber/epoxy interface using dansyl fluorescence, J. Colloid Interface 267 (2003) 117–126.
[28] D. Olmos, A.J. Aznar, J. González-Benito, Kinetic study of the epoxy curing at the silica particles/epoxy interface using the fluorescence of pyrene label, Polym. Test. 24 (2005) 275–283.
[29] J. Gonzalez-Benito, The nature of the structural gradient in epoxy curing at a glass fiber/epoxy matrix interface using FTIR imaging, J. Colloid Interface Sci. 267 (2003) 326–332.